Bulletin of Electrical Engineering and Informatics
Vol. 11, No. 1, February 2022, pp. 239∼247
ISSN: 2302-9285, DOI: 10.11591/eei.v11i1.3137

Outage probability computation in multi-backscatter systems with multi-modes of operation

Dinh-Thuan Do, Anh-Tu Le
Faculty of Electronics Technology, Industrial University of Ho Chi Minh City, Ho Chi Minh City, Vietnam

Article Info

Article history:

Received Jul 14, 2021
Revised Oct 19, 2021
Accepted Dec 29, 2021

Keywords:

Beamforming
Multi-backscatter devices
Non-orthogonal multiple access
Outage probability

ABSTRACT

In this article, we study the outage performance of an ambient multi-backscatter system supported by non-orthogonal multiple access (NOMA) downlink transmission, where legacy users receive information either directly from the base station (BS) or from multiple backscatter devices (BDs) as well. Specifically, we characterize the network connections between the BS and network users into three modes of operation. In the first mode, the BS communicates with the users via the BDs by exploiting NOMA. In the second mode, the BS communicates directly with the users by employing selection combining (SC) beamforming. In the third mode, the users receive signals from both the BS and BDs simultaneously, by using maximal ratio combining (MRC) to combine the BS and BDs links at the users. Consequently, we derive the exact outage expressions of each mode and utilize Monte Carlo simulations to validate the individual exact expressions.

Corresponding Author:

Anh-Tu Le
Faculty of Electronics Technology, Industrial University of Ho Chi Minh City
12 Nguyn Văn Bo, Phng 4, Gò Vp, Thành ph H Chí Minh, Vietnam
Email: leanhtu@iuh.edu.vn

1. INTRODUCTION

The rapid deployment of internet-of-things (IoTs) in diverse systems such as energy systems (Smart Grid), healthcare systems, industrial systems, and transportation systems, has seen a tremendous push into researching ways of powering these billions of devices in a sustainable and environmentally friendly way [1], [2]. Ambient backscatter communication (AmBC) has been proposed by the research community as a solution to address this unique challenge [3]. AmBCs can free up IoT devices from needing batteries as backscatter devices (BDs) harvest energy from traditional radio frequency (RF) transmitters such as television and radio transmitters to transmit information to nearby IoT devices [2]–[13]. Yang *et al*. in [4], the authors note that the harvested energy from ambient RF transmitters is adequate to provide power to high-rate battery-less sensors. Therefore, AmBC can be used in IoT environments where it's not convenient to replace or maintain sensor batteries, e.g., in wide-body area networks (WBANs) [14], [15]. However, due to the broadcast nature of ambient RF transmitters, AmBC tend to suffer from direct-link interference from the RF transmitter [4]–[6]. Several methods such as the design of maximum-likelihood (ML) detectors, and interference cancellation techniques, have been proposed to eliminate the direct-link interference, see [4], [6] and references therein for more details.

In this study, we propose utilizing non-orthogonal multiple access (NOMA) technology to address this problem, owing to its ability to simultaneously serve multiple wireless users over the same radio resource via linear superposition coding at the transmitter and successive interference cancellation (SIC) at the user's receiver [7], [16]–[18]. Therefore, integrating NOMA with AmBC networks shows great promise for future

green IoT networks. Apart from NOMA, there have been several recent studies on deploying reconfigurable intelligent surfaces (RIS) to improve backscatter communication performance [19]–[21]. However, in this article, we focus on the contribution of NOMA to AmBCs performance. Our main contributions are: Firstly, we derive exact outage expressions for three practical AmBC link cases. In the first case, the base station (BS) communicates with the users via the BDs. In the second case, the BS communicates directly with the users. In the third case, the users receive signals from both the BS and BDs simultaneously; Secondly, from these expressions, we analyze the role of channel vectors, power allocation coefficients and backscatter reflection coefficient on outage probability.

All expressions are confirmed using Monte Carlo simulations. The paper is organized is being as. In section 2, we describe the proposed system model and signal characteristics at the users. Thereafter, in section 3, we derive exact outage probability (OP) expressions depending on the mode of operation. In section 4, we explain results, followed by the summary in section 5.

2. RECEIVED SIGNALS AT TWO USERS

In this paper, we study a downlink wireless system to allow the base station (BS) serving two multiple antennas users (user U_1 and user U_2) under assistance of multiple backscatter devices (BDs), shown in Figure 1. In some practical case, the second user U_2 might connect with the BS directly.

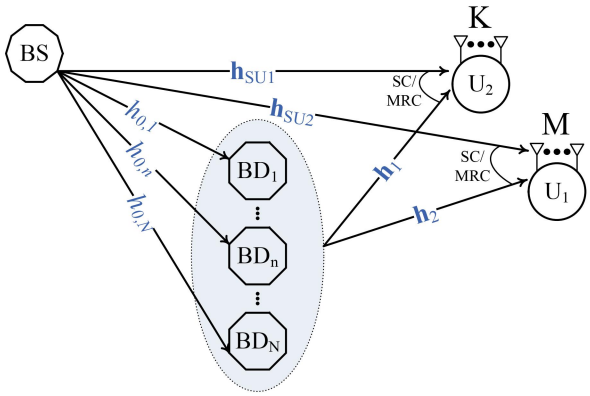

Figure 1. System model of multi-backscatter NOMA

The criteria to choose best multi-backscatter is given by:

$$n = \arg \max_{n=1;2;:::;N} |h_{0;n}|^2: \tag{1}$$

BS broadcasts the information x^{BS} to multi-backscatter (BD_n), $n = 1; 2; : : : N$, which is given by:

$$x^{BS} = \sqrt{a_1 P_S} x_1 + \sqrt{a_2 P_S} x_2; \tag{2}$$

where x_1 and x_2 are the messages with unit power transmitted to U_1 and U_2, respectively. Further, P_S is the total transmit power of the BS with power allocation parameters a_1 and a_2, respectively, with $a_1 > a_2$ and $a_2 + a_1 = 1$.

The maximal-ratio combining (MRC) is used with beamforming vector to achieve optimal transmission scheme as in [22], [23] with $\|w_i\| = 1$:

$$w_i = \frac{h_i^y}{\|h_i\|}; i \in \{1; 2\}; \tag{3}$$

where $\|\cdot\|$ denotes the Euclidean norm of a matrix.

The BD the BS signal to U_1 and U_2 with its own message s, where $\mathbb{E}\{|s|^2\} = 1$. Thus, U_1 and U_2 receive one type of signal: the backscatter link signal from the BD. The received signals at U_1 and U_2 can thus be written as:

$$y_{U_1} = h_{0;n} \|h_1 w_1\| x^{BS} s + n_{U_1}; \quad (4)$$

$$y_{U_2} = h_{0;n} \|h_2 w_1\| x^{BS} s + n_{U_2}; \quad (5)$$

where is a complex reflection coefficient used to normalize, h_1 and h_2 are the $1 \times M$ channel vector of $BD - U_1$ link and $1 \times K$ channel vector of $BD - U_2$ link, n_{U_1} and n_{U_2} are the additive white Gaussian noise (AWGN) with zero mean and variance matrix $^2_{U_1} I_M$ and $^2_{U_2} I_K$, respectively. Hence, the signal x_1 is detected successfully and x_2 as interference. Then, the signal-interference to ratio at U_1 is given by:

$$_{1;1} = \frac{a_1 \ ^2\|h_1\|^2 |h_{0;n}|^2}{a_2 \ ^2\|h_1\|^2 |h_{0;n}|^2 + 1}; \quad (6)$$

where $= \frac{P_S}{^2_{U_i}}$, $i \in \{1; 2\}$ is the transmit signal-to-noise radio (SNR).

Thus, the instantaneous SINR at U_2 to detect x_1 and the instantaneous SNR at U_2 to detect x_2 is given respectively as:

$$_{2;1} = \frac{a_1 \ ^2\|h_2\|^2 |h_{0;n}|^2}{a_2 \ ^2\|h_2\|^2 |h_{0;n}|^2 + 1}, \quad _{2;2} = a_2 \ ^2\|h_2\|^2 |h_{0;n}|^2. \quad (7)$$

3. OUTAGE PROBABILITY COMPUTATION OF DIFFERENT MODES

3.1. Scheme 1: outage probability for backscatter-non-orthogonal multiple access system without direct link

In this study, we assume independent Rayleigh-distributed random variables (RVs) for all the channels. Thus, RVs $|h_{0;n}|^2$, $\|h_i\|^2$ have exponential distributions, with $f_{|h_{0;n}|^2}(x) = \sum_{n=1}^{N} \binom{N}{n} \frac{n(-1)^{n-1}}{h_0} e^{-\frac{nx}{h_0}}$, $f_{k\mathbf{h}_i k^2}(x) = \frac{x^{N-1} e^{-\frac{x}{h_i}}}{(N)\ ^N_{h_i}}$ and $F_{k\mathbf{h}_i k^2}(x) = 1 - e^{-\frac{x}{h_i}} \sum_{p=0}^{N-1} \frac{x^p}{(p+1)\ ^p_{h_i}}$ with $(x) = (x-1)!$ is the gamma function.

The OP of U_1 is:

$$\mathcal{OP}^I_{U_1} = \Pr(_{1;1} < _1); \quad (8)$$

where $_1 = 2^{R_1} - 1$ with R_1 being the target rate at U_1 to detect x_1.

Theorem 1. *The exact OP expression of U_1 is calculated as*:

$$\mathcal{OP}^I_{U_1} = 1 - 2 \sum_{m=0}^{M-1} \sum_{n=1}^{N} \binom{N}{n} \frac{(-1)^{n-1} \binom{m}{1} n}{(m+1)\ ^m_{h_1} h_0} \times \left(\frac{1 \ h_0}{h_1 n}\right)^{\frac{1+m}{2}} K_{1+m}\left(2\sqrt{\frac{_1 n}{h_1 h_0}}\right); \quad (9)$$

where $_1 = \frac{1}{(a_1 \ _1 a_2)}$. Note (9) is based on the condition of $a_1 > \ _1 a_2$

Proof:

$$\begin{aligned}
\mathcal{OP}^I_{U_1} &= 1 - \Pr\left(\|h_1\|^2 > \frac{1}{^2|h_{0;n}|^2}\right) \\
&= 1 - \int_0^{+\infty} F_{k h_1 k^2}\left(\frac{1}{^2 t}\right) f_{|h_{0;n}|^2}(t)\, dt \\
&= 1 - \sum_{m=0}^{M-1} \sum_{n=1}^{N} \binom{N}{n} \frac{(-1)^{n-1} \binom{m}{1} n}{(m+1)\ ^m_{h_1}\ ^{2m}_{\ h_0}} (t);
\end{aligned} \quad (10)$$

where $F_{k\mathbf{h}_1 k^2}(x) = 1 - F_{k\mathbf{h}_1 k^2}(x)$ and $(t) = \int_0^{\infty} e^{-\frac{1}{2}\frac{1}{h_1 t} - \frac{nt}{h_0}} t^{m} dt$.

Based on [24], (3.471.9). We can rewrite (10) as:

$$\mathcal{OP}^{I}_{U_1} = 1 - 2\sum_{m=0}^{M-1}\sum_{n=1}^{N} \binom{N}{n} \frac{(-1)^{n-1}\, {}_1^{m} n}{(m+1)!\, {}_{h_1}^{m}\, {}_{2}^{2}\, {}_{h_0}} \times \left(\frac{1}{2}\frac{h_0}{{}_{h_1} n}\right)^{\frac{1+m}{2}} K_{1+m}\left(2\sqrt{\frac{{}_1 n}{{}_{h_1}{}_{2}{}_{h_0}}}\right); \tag{11}$$

Next, the OP of U_2 is given by:

$$\mathcal{OP}^{I}_{U_2} = \Pr({}_{2;2} < {}_2) = 1 - \Pr\left(\|\mathbf{h}_2\|^2 |h_{0;n}|^2 > {}_2\right); \tag{12}$$

where ${}_2 = 2^{R_2} - 1$ with R_2 being the target rate at U_2 to detect x_2, ${}_2 = \frac{{}_2}{a_2}$. Similarly with solving $\mathcal{OP}^{I}_{U_1}$ can be achieved $\mathcal{OP}^{I}_{U_2}$ as:

$$\mathcal{OP}^{I}_{U_2} = 1 - 2\sum_{k=0}^{K-1}\sum_{n=1}^{N} \binom{N}{n} \frac{(-1)^{n-1}\, {}_2^{k} n}{(k+1)!\, {}_{h_2}^{k}\, {}_{2k}\, {}_{h_0}} \times \left(\frac{2}{2}\frac{h_0}{{}_{h_2} n}\right)^{\frac{1+k}{2}} K_{1+k}\left(2\sqrt{\frac{2}{{}_{h_2}{}_{2}{}_{h_0}}}\right); \tag{13}$$

3.2. Scheme 2: outage probability of directed link by selection combining mode

In the MRT scheme, to maximize the signal-to-interference noise (SINR) at U_1 and U_2, BS uses a beamforming transmit vector $w_r = \frac{h_r^{y}}{k h_r k}$, $r \in \{SU_1; SU_2\}$ to signal x^{BS} before sending w_r to users, h_{SU_1} and h_{SU_2} are the $1 \times M$ and $1 \times K$ channel vector of BS to U_1 link and BS to U_2 link, respectively. The BS transmits signals directly to two users as

$$y_r = \|h_r w_r\| x^{BS} + n_r \quad ; r \in \{SU_1; SU_2\}: \tag{14}$$

We have SINR at U_1 as:

$${}_{SU_1} = \frac{\|h_{SU_1}\|^2 a_1}{\|h_{SU_1}\|^2 a_2 + 1}; \tag{15}$$

and SINR and the successive interference cancellation (SIC) at U_2 as ${}_{SU_{2;1}} = \frac{\|h_{SU_2}\|^2 a_1}{\|h_{SU_2}\|^2 a_2 + 1}$ and U_2 as ${}_{SU_2} = \|h_{SU_2}\|^2 a_2$, respectively.

Finally, the instantaneous SINRs at U_1 and U_2 based on selection combining, can be written as:

$${}^{SC}_{i} = \Pr(\max({}_{SU_i}; {}_{i;i}) < {}_i) \quad ; i \in \{1; 2\} \tag{16}$$

The OP of U_1 is given by:

$$\begin{aligned} F_{{}_{1;1}}(x) &= \Pr\left(\|h_1\|^2 < \frac{x}{(x)|h_{0;n}|^2}\right) \\ &= 1 - \int_0^{\infty} F_{k\mathbf{h}_1 k^2}\left(\frac{x}{(x)t}\right) f_{|h_{0;n}|^2}(t)\, dt \\ &= 1 - \sum_{m=0}^{M-1}\sum_{n=1}^{N} \binom{N}{n} \frac{n x^{m} (-1)^{n-1}}{(m+1)!\, {}_{h_1}^{m}\, {}_{h_0}\, (x)^{m}} (t|x); \end{aligned} \tag{17}$$

where $(t|x) = \int_0^{\infty} e^{-\frac{x}{h_1 (x)t} - \frac{nt}{h_0}} t^{m} dt$ and $(x) = (a_1 - x a_2)^{2}$. Using [24], (3.471.9) and after some transform. $F_{{}_{1;1}}(x)$ and $F_{{}_{SU_2}}(x)$ can be express respectively as:

$$F_{{}_{1;1}}(x) = 1 - 2\sum_{m=0}^{M-1}\sum_{n=1}^{N} \binom{N}{n} \frac{n x^{m} (-1)^{n-1}}{(m+1)!\, {}_{h_1}^{m}\, {}_{h_0}\, (x)^{m}} \times \left(\frac{x}{h_1}\frac{h_0}{(x)}\right)^{\frac{1+m}{2}} K_{1+m}\left(2\sqrt{\frac{xn}{{}_{h_1}{}_{h_0}(x)}}\right); \tag{18}$$

and,

$$F_{_{SU_1}}(x) = 1 - \sum_{m=0}^{M-1} \frac{x^m e^{\frac{x}{(a_1 - xa_2)\ _{SU_1}}}}{(m+1)\ {}^m_{SU_1}(a_1 - xa_2)^m\ {}^m}. \tag{19}$$

Substituting (18) and (19) into (16), the close-form of OP of $\mathcal{OP}^{I\,I}_{U_1}$ is obtained as:

$$\mathcal{OP}^{\mathcal{II}}_{U_1} = \left[1 - 2\sum_{m=0}^{M-1}\sum_{n=1}^{N}\binom{N}{n}\frac{n\gamma_1^m(-1)^{n\ 1}}{(m+1)\ {}^m_{h_1}\ h_0{}^n(\gamma_1)^m}\left(\frac{\gamma_1\ h_0}{h_1(\gamma_1)}\right)^{\frac{1\ m}{2}} K_{1-m}\left(2\sqrt{\frac{\gamma_1 n}{h_1\ h_0(\gamma_1)}}\right)\right] \times \left[1 - \sum_{m=0}^{M-1}\frac{\theta_1^m e^{\frac{1}{SU_1}}}{(m+1)\ {}^m_{SU_1}}\right]. \tag{20}$$

Next, the OP of U_2 is:

$$\mathcal{OP}^{I\,I}_{U_2} = \Pr\left(\ {}^{SC}_{2} < \ _2\right) = \Pr\left(\ _{SU_2} < \ _2\right)\Pr\left(\ _{2;2} < \ _2\right). \tag{21}$$

Similarly, $\mathcal{OP}^{I\,I}_{U_2}$ can be achieved as:

$$\mathcal{OP}^{I\,I}_{U_2} = \left(1 - 2\sum_{k=0}^{KP\ 1}\sum_{n=1}^{N}\binom{N}{n}\frac{n\ _2{}^k(\ 1)^{n\ 1}}{(m+1)\ {}^k_{h_2}\ h_0{}^{2k}} \times \frac{_2\ h_0}{h_2\ {}^2n}^{\frac{1\ k}{2}} K_{1\ k}\ 2\sqrt{\frac{}{{}_2{}^2n}{h_2\ {}^2\ h_0}}\right) \times \left(1 - e^{\frac{}{SU_2}}\sum_{k=0}^{KP\ 1}\frac{}{(k+1)\ {}^k_{SU_2}}\right). \tag{22}$$

3.3. Scheme 3: outage probability of directed link by maximal ratio combining mode

In this scheme, the backscattering link signals and direct link signals are combined by maximal ratio combining (MRC) at the two users. Hence, after using MRC the received SINR two users are given by:

$$\ {}^{MRC}_{U_i} = \ _{SU_i} + \ _{i;i} \quad ; i \in \{1; 2\} \tag{23}$$

Then, the OP at U_1 can be calculated as:

$$\begin{aligned}\mathcal{OP}^{I\,I\,I}_{U_1} &= \Pr\left(\ _{SU_1} < \ _1 - \ _{1;1}\right)\\ &= \int_0^{Z^1}\int_0^{Z\ x} f_{\ _{1;1}}(x)\ f_{\ _{SU_1}}(y)dydx.\end{aligned} \tag{24}$$

It is very difficult to obtain the close-form solution of the integral of (24). Therefore, we use the approach in [25] by making an I-step staircase approximation to the actual triangular integral region in (24) with sufficiently large I to obtain:

$$\mathcal{OP}^{I\,I\,I}_{U_1} \approx \sum_{i=0}^{KP\ 1} F_{\ _{SU_1}}\left(\frac{i+1}{I}\ 1\right) - F_{\ _{SU_1}}\left(\frac{i}{I}\ 1\right) \times F_{\ _{1;1}}\left(\frac{I-i}{I}\ 1\right). \tag{25}$$

Thus, the OP at U_2 is given by:

$$\begin{aligned}\mathcal{OP}^{I\,I\,I}_{U_2} &= \Pr\left(\ {}^{MRC}_{U_2} < \ _2\right)\\ &= \int_0^{Z^2} f_{\|\mathbf{h}_{SU_2}\|^2}(x)F_{k\mathbf{h}_2k^2|h_{0,n}\ |^2}\left(\frac{2}{2} - \frac{x}{2}\right)dx\\ &= \frac{1}{(K)\ {}^K_{h_{SU_2}}}[\ _1 - \ _2];\end{aligned} \tag{26}$$

where $_2 = \frac{2}{a_2}$. $_1$ can be calculated as:

$$_1 = \int_0^{R} x^{K\ 1} e^{\frac{x}{h_{SU_2}}} dx = \ K; \frac{2}{h_{SU_2}} \ ; \tag{27}$$

where $(x; y)$ is the lower incomplete Gamma function [24], (3.351.1). And $_2$ is written as:

$$_2 = 2 \sum_{n=1}^{N} \sum_{k=0}^{K\ 1} \binom{N}{n} \frac{n^{(k+1)/2} \ (\ 1)^{n\ 1}}{(k+1)} \frac{}{h_0^{(k+1)/2} \ h_2^{(k+1)/2}} \int_0^{Z_2} x^{K\ 1} e^{\frac{x}{h_{SU_2}}} \ \frac{2}{2} \ \left(\frac{x}{2}\right)^{(k+1)/2} \ s \ \frac{}{K_{1\ k}\ 2 \sqrt{\frac{n}{h_0 \ h_2}} \ \frac{2}{2} \ \frac{x}{2}} dx; \tag{28}$$

Putting $t = 2x/ \ _2 \ 1) \ _2 (t + 1)/2 = x) \ _2/2 \, dt = dx$. But it is very dif cult to obtain the close-form solution of $_2$, to do so, we use Gaussian-Chebyshev quadrature [26], (25.4.38), to get:

$$_2 \ \frac{}{2} \sum_{n=1}^{N} \sum_{k=0}^{K\ 1} \sum_{l=1}^{L} \binom{N}{n} \frac{n^{(k+1)/2} \ (\ 1)^{n\ 1} \ _2^K}{h_0^{(k+1)/2} \ h_2^{(k+1)/2} \ 2^{K\ 1}} \frac{\sqrt{1 \ _l^2} (\ _l+1)^{K\ 1} (\ _l)^{(k+1)/2}}{(K) \ h_{SU_2}^{K} \ (k+1) L} \ q \frac{}{K_{1\ k}\ 2 \frac{n(\ _l)}{h_0 \ h_2}} : \tag{29}$$

Substituting (26) and (28) into (25), $OP_{U_2}^{III}$ is given by:

$$OP_{U_2}^{III} \ \frac{K; \frac{}{2} \ h_{SU_2}}{(K)} \sum_{n=1}^{N} \sum_{k=0}^{K\ 1} \sum_{l=1}^{L} \binom{N}{n} \frac{n^{(k+1)/2} \ (\ 1)^{n\ 1} \ _2^K}{h_0^{(k+1)/2} \ h_2^{(k+1)/2} \ 2^{K\ 1}} K_{1\ k}\ 2 \sqrt{\frac{n(\ _l)}{h_0 \ h_2}} \frac{\sqrt{1 \ _l^2} (\ _l+1)^{K\ 1} (\ _l)^{(k+1)/2}}{(K) \ h_{SU_2}^{K} \ (k+1) L} e^{\frac{2(\ _l+1)}{2 \ h_{SU_2}}} ; \tag{30}$$

where $_l = \cos \frac{2l \ 1}{2L}$ and $(x) = \frac{2}{2} \ \frac{2(x+1)}{2 \ 2}$.

4. NUMERICAL RESULTS

In this section, we set $d_0 = d_1 = d_{SU_1} = d_{SU_2} = 1$, $d_2 = 2$, $h_0 = d_0$, $h_1 = d_1$, $h_2 = d_2$, $_{SU_1} = d_{SU_1}$ and $_{SU_1} = d_{SU_1}$ and is the path-loss exponent setting to be = 2. In particular, main parameters can be seen in Table 1. In addition, the Gauss-Chebyshev parameter is selected to be L = 10 to yield a close approximation.

Table 1. System parameters used in the performance evaluation

System Parameters	Values
Monte Carlo simulations repeated	10^7 iterations
The power allocation coef cients	$f a_1; a_2 g = f 0:8; 0:2g$
The target rate at U_1	$R_1 = 2$ bps/Hz
The target rate at U_2	$R_2 = 2$ bps/Hz
The complex re ection coef cient	$= 0 :5$

Figure 2 plots OP and base station transmit SNR relationship, with with varying $N = K = M = 1$ and $N = K = M = 3$. In (8), (12), (19), (20), (23), and (29) are used to plot the analytical lines. From Figure 2, we notice that the network users experience different outage performances depending on the $N = K = M$ values. The best performances are achieved by scheme 3, with the worst performance obtained by scheme 1. We can see the analytical curves t with Monte Carlo simulations.

Figure 3 plots the OP relationship between outage and base station transmit SNR, with varying = 0:3 and = 0:7. As in Figure 2, from Figure 3, we also observe that the users experience different outage performances depending on the complex re ection coef cient. The best performances are achieved by scheme 3, with the worst performance obtained by user 2 in scheme 1.

Figure 4 plots the relationship between OP and = $_1$ (dB), varying = 0:3, and = 0:7. From Figure 4, we observe that some network users performance curves approach an outage probability ceiling. Generally, the outage performance reduces with increase in = $_1$ (dB). The best performances are achieved by scheme 3, with the worst performance obtained by scheme 1.

Figure 2. Outage probability versus (dB) varying N = K = M = 1 and N = K = M = 3

Figure 3. Outage probability versus (dB) varying = 0:3 and = 0:7

Figure 4. Outage probability versus = $_1$ (dB) varying = 0:3 and = 0:7

Figure 5 plots the relationship between OP and power allocation coef cient, varying N = K = M = 1 and N = K = M = 2 with = 20 (dB) and $R_1 = R_2 = 1$. From Figure 5, we note that several OP curves approach an OP oor with increasing , while other OP curves converge at 0 when = 1. Figure 6 plots the relationship between OP and N = M = K, with = 5 (dB). From Figure 5, we observe that maximal ratio combining delivers the best outage performance with the OP for backscatter-NOMA system performing the worst. In both Figures, user 2 in scheme 1 had the worst OP performance, due to the weak backscatter device signals that it recovers, therefore, it can easily experience outage in any condition. With user 1 in scheme 3 achieving the best performance due to the signals from the very near multi-backscattering devices and the further away base station direct link being combined by maximal ratio combining at its receiver.

Figure 5. Outage probability versus a_2 varying $N = K = M = 1$ and $N = K = M = 2$ with $= 20$ (dB) and $R_1 = R_2 = 1$

Figure 6. Outage probability versus $N = M = K$ with $= 5$ (dB)

5. CONCLUSION

In this paper, we provided the outage probability (OP) analysis of an ambient multi-backscatter system with multi-modes of operation. We derived exact solutions of OP for different users depending on the mode of operation. We observe from the simulation results, that the direct link between the base station and users affects the OP. In future work, we will consider ergodic capacity of the system.

REFERENCES

[1] H. Jayakumar, K. Lee, W.S. Lee, A. Raha, Y. Kim, and V. Raghunathan, "Powering the internet of things," in Proceedings of the 2014 international symposium on Low power electronics and design, pp. 375–380, 2014, doi: 10.1145/2627369.2631644.
[2] F. Jameel, S. Zeb, W. U. Khan, S. A. Hassan, Z. Chang, and J. Liu, "NOMA-Enabled Backscatter Communications: Toward Battery-Free IoT Networks," in IEEE Internet of Things Magazine, vol. 3, no. 4, pp. 95–101, 2020, doi: 10.1109/IOTM.0001.2000055.
[3] N. Van Huynh, D. T. Hoang, X. Lu, D. Niyato, P. Wang, and D. I. Kim, "Ambient Backscatter Communications: A Contemporary Survey," in IEEE Commun. Surv. & Tutor., vol. 20, no. 4, pp. 2889-2922, 2018, doi: 10.1109/COMST.2018.2841964.
[4] G. Yang, Y. -C. Liang, R. Zhang, and Y. Pei, "Modulation in the Air: Backscatter Communication Over Ambient OFDM Carrier," in IEEE Transactions on Communications, vol. 66, no. 3, pp. 1219-1233, March 2018, doi: 10.1109/TCOMM.2017.2772261.
[5] W. Zhao, G. Wang, R. Fan, L. Fan, and S. Atapattu, "Ambient Backscatter Communication Systems: capacity and Outage Performance Analysis," in IEEE Access, vol. 6, pp. 22695-22704, 2018, doi: 10.1109/ACCESS.2018.2828021.
[6] G. Yang, Q. Zhang, and Y. Liang, "Cooperative Ambient Backscatter Communications for Green Internet-of-Things," in IEEE Internet of Things Journal, vol. 5, no. 2, pp. 1116-1130, April 2018, doi: 10.1109/JIOT.2018.2799848.
[7] Q. Zhang, L. Zhang, Y. Liang, and P. Kam, "Backscatter-NOMA: A Symbiotic System of Cellular and Internet-of-Things Networks," in IEEE Access, vol. 7, pp. 20000-20013, 2019, doi: 10.1109/ACCESS.2019.2897822.
[8] B. Lyu, Z. Yang, G. Gui, and Y. Feng, "Wireless Powered Communication Networks Assisted by Backscatter Communication," in IEEE Access, vol. 5, pp. 7254-7262, 2017, doi: 10.1109/ACCESS.2017.2677521.